

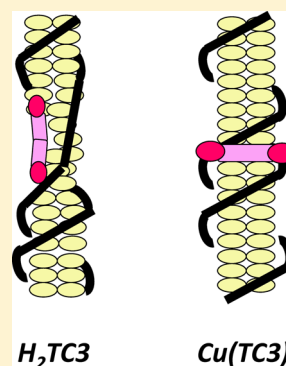
## DNA-Binding Studies of a Tetraalkyl-Substituted Porphyrin and the Mutually Adaptive Distortion Principle

Srijana Ghimire, Phillip E. Fanwick, and David R. McMillin\*

Department of Chemistry, Purdue University, 560 Oval Drive, West Lafayette, Indiana 47907, United States

## Supporting Information

**ABSTRACT:** This investigation explores DNA-binding interactions of various forms of an alkyl-substituted cationic porphyrin, H<sub>2</sub>TC3 (5,10,15,20-tetra[3-(3'-methylimidazolium-1'-yl)]-porphyrin). The motivating idea is that incorporating alkyl rather than aryl substituents in the meso positions will enhance the prospects for intercalative as well as external binding to DNA hosts. The ligands may also be applicable for photodynamic and/or anticancer therapy. Methods employed include absorbance, circular dichroism, and emission spectroscopies, as well as viscometry and X-ray crystallography. By comparison with the classical H<sub>2</sub>T4 system, H<sub>2</sub>TC3 exhibits a higher molar extinction coefficient but is more prone to self-association. Findings of note include that the copper(II)-containing form Cu(TC3) is adept at internalizing into single-stranded as well as B-form DNA, regardless of the base composition. Surprisingly, however, external binding of H<sub>2</sub>TC3 occurs within domains that are rich in adenine–thymine base pairs. The difference in the deformability of H<sub>2</sub>TC3 versus Cu(TC3) probably accounts for the reactivity difference. Finally, Zn(TC3) binds externally, as the metal center remains five-coordinate.

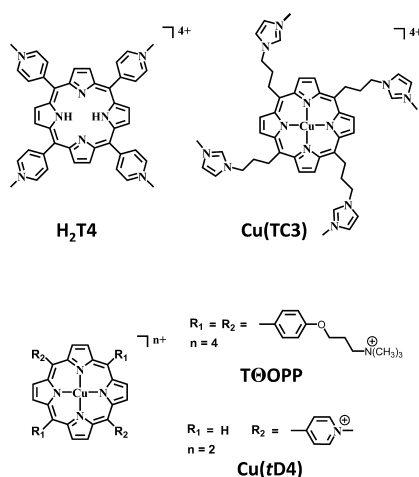


## INTRODUCTION

The aim of this investigation was to explore the DNA-binding interactions of new cationic porphyrins with alkyl functional groups in the meso positions. The present dearth of studies dealing with alkyl-substituted forms is surprising in light of the long history of DNA-binding studies with aryl-substituted porphyrins, most especially the H<sub>2</sub>T4 system depicted in Chart 1.<sup>1–3</sup> Cationic porphyrins like H<sub>2</sub>T4 are useful because they enter cells readily.<sup>4,5</sup> They also exhibit prominent absorption in the red end of the visible system, which means they can function as sensitizers for photodynamic therapy.<sup>6–8</sup> One application could be for topical antibacterial treatment.<sup>9</sup> Being

telomerase inhibitors as well, cationic porphyrins also have potential applications in anticancer therapies.<sup>10,11</sup> Research has established that the porphyrin ligands adopt at least three distinct binding motifs when interacting with double-stranded (ds) DNA hosts.<sup>1,2,12</sup> The mode of binding is usually evident from physical studies. For example, intercalation between base pairs typically gives rise to a bathochromic shift of 10–15 nm in the Soret region and a hypochromic response of about 30%. In the same spectral region it also gives rise to an induced circular dichroism (iCD) having a negative sign. In contrast, external binding generally gives rise to a positive iCD signal, a smaller bathochromic shift, and a much weaker, or even negative hypochromic response. Finally, some very hydrophobic porphyrins, such as T<sup>+</sup>OPP in Chart 1, bind by aggregating and/or stacking on the surface of the DNA host.<sup>1,13,14</sup> External stacking often induces a conservative, sometimes very intense bisignate iCD signal in the Soret region of the visible spectrum.<sup>15</sup> The factors that influence the choice of binding motif are becoming clearer. The amphiphilic nature of the ligand seems ideally suited for intercalative binding, which allows the hydrophobic core to sandwich between DNA bases with positively charged substituent groups of the porphyrin extending outward toward the sugar–phosphate backbones of the DNA host and into solution. With this mode of binding the Watson–Crick hydrogen-bonding framework of the host also remains intact. However, steric forces also come into play. If, for example, the central metal of a metallocporphyrin retains one or more axial ligands, intercalative binding is no longer

Chart 1



Received: July 14, 2014

possible.<sup>3</sup> An X-ray structural study has also established that intercalation of Cu(T4) inevitably leads to clashes in the minor groove involving the bulky *N*-methylpyridiniumyl substituents of the porphyrin and backbone residues of the host.<sup>16</sup> Accordingly, Cu(T4) and its analogues only intercalate into G≡C-rich domains where hydrogen bonding is strong, and the duplex structure is durable.<sup>3,17–19</sup> The alternative is external binding, but H<sub>2</sub>T4 has an extended structure with a rigidly disposed charge distribution. At least in part for that reason high-affinity external binding therefore requires significant reorganization of the DNA structure and formation of a suitable binding pocket.<sup>13,20</sup> As a consequence external binding is most feasible in A=T-rich domains, which have a weaker hydrogen-bonding framework and a lower melting temperature.

Many variants of H<sub>2</sub>T4 have been explored. Early on, for example, Sari et al. systematically tuned the charge by replacing *N*-methylpyridiniumyl groups with phenyl groups.<sup>21</sup> Not surprisingly, they found that reducing the charge also lowers the binding affinity. Others have kept the charge constant while enhancing the hydrophobic character by incorporating additional aromatic groups in the meso substituents.<sup>22</sup> Neither approach addresses two basic limitations, however. The first is that aromatic substituents are rigid as well as bulky, giving rise to previously mentioned steric clashes in the minor groove.<sup>16</sup> Second, periplanar interactions involving the  $\beta$  hydrogens of the porphyrin ring require the substituents to orient essentially perpendicularly with respect to the plane of the porphyrin.<sup>23</sup> That, in turn, can inhibit stacking with DNA bases, particularly when the host site has a large footprint, as is the case with a leaflet of G-quadruplex DNA.<sup>11</sup> Another approach involves decreasing the number of *N*-methylpyridiniumyl substituents, thereby reducing the steric problems.<sup>24–27</sup> This approach has worked quite well, and Cu(tD4) and Pd(tD4) turn out to be universal intercalators for B-form DNA (Chart 1).<sup>26,28,29</sup> In other words, both ligands bind by intercalation regardless of the base composition of the DNA. One of the most intriguing observations is that Pd(tD4) is superior to H<sub>2</sub>T4 analogues in sensitizing the formation of singlet oxygen.<sup>29</sup> A downside is that trimming the number of substituents reduces the net charge and the solubility of the ligand in aqueous solution. In the design adopted herein the ligand retains a net charge of 4+. The motivation behind incorporating alkyl substituents is at once to reduce the effective size of the porphyrin and develop a form that is more conducive to stacking with DNA bases. In future work it will also be possible to vary the nature of the charging groups as well as the length of the tether. Here, the focus is on H<sub>2</sub>TC3 and metal-containing derivatives, where H<sub>2</sub>TC3 denotes 5,10,15,20-tetra[3-(3'-methylimidazolium-1'-yl)]porphyrin; see Chart 1 for a view of the copper(II)-containing form Cu(TC3). The binding studies reported herein employ single- and double-stranded (ds) DNA hosts. The ds hosts include salmon testes DNA as well as a series of hairpin-forming oligonucleotides, vide infra, which have stems that vary in base composition. Interestingly, Cu(TC3) and H<sub>2</sub>TC3 tend to adopt different binding motifs, even though each is a nominally planar porphyrin. With every host investigated Cu(TC3) binds strictly by intercalation, whereas external binding of H<sub>2</sub>TC3 becomes an increasingly competitive process as the percentage of A=T base pairs increases in the host. The difference in the deformability of the two forms presumably accounts for the change in the mode of binding. High-affinity external binding requires a significant reorganization of the

host, and a ligand that can undergo a mutually adaptive distortion (MAD) enhances the induced fit.

## ■ EXPERIMENTAL SECTION

**Materials.** Hexanes, dichloromethane (DCM), dimethylformamide (DMF), acetone, methanol (MeOH), toluene, acetonitrile (MeCN), and potassium nitrate (KNO<sub>3</sub>) were products of Mallinckrodt Chemicals. Macron Chemicals supplied acetic acid and nitric acid, but the hydrochloric acid came from J. T. Baker. Silica was a product of Sorbent Technologies, whereas alumina was from EMD Chemicals. Integrated DNA Technologies was the provider for both single-stranded (ss) and hairpin-forming DNA (ds) sequences. The sequences obtained were 5'-GATTACtttGTAATC-3' (GATTAC), 5'-GACGACtttGTCGTC-3' (GACGAC), 5'-GCGCACtttGTGCGC-3' (GCGCAC), and 5'-AGCGACtttGTCGCT-3' (AGCGAC), where lower case letters designate bases involved in loop formation. Similarly the ss sequences were 5'-TCCTGCCACGCTCCGC-3' (Puc) and 5'-TTTTTTTTTT-3' (T<sub>10</sub>). Indium(III) chloride, trizma chloride, trizma base, pyrrole, tetrabutylammonium nitrate (TBAN), potassium hexafluorophosphate (KPF<sub>6</sub>), silica thin-layer chromatography (TLC) plates, and silanizing solution (5% dichlorodimethylsilanes in *n*-heptane) were products of Sigma-Aldrich Commercial. Other materials supplied by Sigma-Aldrich included 4-chloro-1-butanol, 1-methylimidazole, pyridinium chlorochromate (PCC), *para*-toluenesulfonic acid (PTSA-H<sub>2</sub>O), 2,3,5,6-tetrachloro-1,4-benzoquinone (TCQ), copper acetate (Cu(OAc)<sub>2</sub>), Zn(OAc)<sub>2</sub>, KMnO<sub>4</sub>, and salmon testes (ST) DNA with an average length of 300 base pairs.

**Synthesis.** *4-Chlorobutanol.* Commercially available 4-chloro-1-butanol reacts with PCC in anhydrous DCM at room temperature to give 4-chlorobutanol.<sup>30</sup> Because of poor solubility it helps to suspend the PCC in DCM about 20 min before the addition of the alcohol. TLC on silica with elution with 2:1 hexane/diethyl ether is a good way of monitoring the progress of reaction. Dipping the TLC plate into a KMnO<sub>4</sub> solution and drying with a heat gun reveals two spots with different retention factor values. Complete conversion of the *R*<sub>f</sub> spot of alcohol into the faster-moving *R*<sub>f</sub> spot of aldehyde indicates the completion of the reaction. <sup>1</sup>H NMR in CDCl<sub>3</sub>: 9.94 ppm (s, 1H), 3.73 ppm (t, 2H), 2.80 ppm (m, 2H), 2.23 ppm (t, 2H).

*H<sub>2</sub>TC3.* The first step in the synthesis of 5,10,15,20-tetra-(3-chloropropyl)porphyrin (H<sub>2</sub>TC3) is the condensation of 4-chlorobutanol with pyrrole in the presence of *p*-toluene sulfonic acid as catalyst. The second step is oxidation with TCQ at ~110 °C.<sup>32</sup> A Dean–Stark trap is present to collect the water and maintain anhydrous conditions. Absorption spectroscopy and TLC on silica with 1:1 hexane/ethyl acetate are useful for following reaction progress. Column chromatography (elution from silica with 3:1 hexane/ethyl acetate) is the main purification step. The dark pink, slow-moving band is the desired product. <sup>1</sup>H NMR in CDCl<sub>3</sub>: 9.53 ppm (s, 8H), 5.12 ppm (m, 8H), 3.87 ppm (m, 8H), 2.97 ppm (m, 8H), –2.79 ppm (s, 2H).

Substitution of chloro groups with 1-methyl imidazole by the method of Wu et al. gives the desired tetra-cationic product 5,10,15,20-tetra[(3-(3'-methylimidazolium-1'-yl)propyl)]porphyrin (H<sub>2</sub>TC3).<sup>33</sup> The reaction requires about a week to complete. Column chromatography (silica in 8% MeCN, 10% aqueous KNO<sub>3</sub>, and 10% deionized H<sub>2</sub>O) allows separation from incompletely modified porphyrin.<sup>34</sup> The slowest-moving band corresponds to the desired tetracation. After evaporation of solvents, aqueous KPF<sub>6</sub> addition precipitates the porphyrin from acetonitrile. Ion exchange to the nitrate salt is possible by dissolving the hexafluorophosphate salt in acetonitrile followed by precipitating with a solution of tetrabutylammonium nitrate in acetone. Vapor diffusion of tetrahydrofuran into a solution of either the nitrate in methanol or the hexafluorophosphate form in acetonitrile gives small crystals of the desired product.

**Analysis.** Anal. Calcd for C<sub>48</sub>H<sub>58</sub>F<sub>24</sub>N<sub>12</sub>P<sub>4</sub>: C 41.69, H 4.23, and N 12.15%; found: C 40.81, H 4.17, and N 12.35%. <sup>1</sup>H NMR in deuterated dimethyl sulfoxide: 9.74 ppm (s, 8H), 9.22 ppm (d, 4H),

7.96 ppm (d, 4H), 7.78 ppm (d, 4H), 5.05 ppm (m, 8H), 4.74 ppm (m, 8H), 3.87 ppm (m, 12H), 2.93 ppm (t, 8H).

**Cu(TC3).** Dissolving the nitrate salt of H<sub>2</sub>TC3 in 50/50 MeOH/H<sub>2</sub>O (v/v) and treating with dilute acid removes any traces of zinc(II) from the porphyrin.<sup>29</sup> Addition of aqueous KPF<sub>6</sub> solution precipitates the porphyrin. Metal insertion occurs upon exposure to copper acetate in DMF for 12 h. It is possible to monitor reaction progress by absorption and emission spectroscopy. Metal insertion increases the symmetry of a molecule and reduces the number of Q bands from four to two. The emission signal drops to zero in DMF with the formation of Cu(TC3). Anal. Calcd for C<sub>48</sub>H<sub>58</sub>CuF<sub>24</sub>N<sub>12</sub>P<sub>4</sub>: C 39.91, H 3.91 and N 11.64%; found: C 40.01, H 4.00, and N 11.51%.

**Zn(TC3).** Addition of 2 equiv of zinc acetate in water to a solution of the hexafluorophosphate salt of H<sub>2</sub>TC3 in an equal volume of acetonitrile leads to the formation of the zinc derivative of the porphyrin. Absorption spectroscopy is once again useful for monitoring the reaction progress, and insertion is complete when only two Q bands are present.

**Methods.** Silanization of the glassware minimized porphyrin absorption on surfaces.<sup>35</sup> In titrations, the porphyrin concentration remained constant at 1.00 μM, and only the DNA concentration changed. In the absence of DNA host, the medium used for measuring spectra of porphyrins was pure methanol to avoid aggregation. But when DNA was present in the sample, the only source of methanol was a small amount introduced with the porphyrin stock solution. Beer's law studies yielded the molar extinction coefficients of the porphyrins, needed for calibrating all stock solutions. For consistency with the ST host, the unit of DNA used for the hairpins is a base pair. Thus, the molar extinction coefficients for the hairpin hosts in Table 1

**Table 1. List of Molar Extinction Coefficients<sup>a</sup>**

species	$\epsilon$ (260 nm, M <sup>-1</sup> cm <sup>-1</sup> )
double-stranded hosts	
GATTAC	18 300
GACGAC	18 300
GCGCAC	17 200
AGCGCA	18 600
ST	13 200 <sup>36</sup>
single-stranded hosts	
Puc	130 300 <sup>b</sup>
T <sub>10</sub>	81 600 <sup>b</sup>
porphyrins	
H <sub>2</sub> TC3 <sup>c</sup>	$5.45 \times 10^5$
Cu(TC3) <sup>d</sup>	$6.00 \times 10^5$

<sup>a</sup>Base-pair units except for the ss hosts. <sup>b</sup>Strand basis. <sup>c</sup>Soret wavelength of 413 nm. <sup>d</sup>Soret wavelength of 412 nm.

are the strand values quoted by the supplier divided by 8. In contrast, for an ss host the unit of DNA is the complete strand. For each step in a titration,  $q$  designates the ratio of the host concentration to that of the porphyrin. To facilitate equilibration of the sample during a serial titration, for each value of  $q$  the procedure was to add half the volume of buffer needed, followed in order by aliquots of salt solution, DNA, and porphyrin before adding the rest of the buffer. The buffer for the binding studies was pH = 7.5 Tris-chloride. The solutions contained 0.05 M chloride from the buffer and 0.10 M NaCl, or 0.05 M NaCl in the case of viscometry runs.

Equation 1 yielded the percent hypochromism (%  $H$ ), where  $A(\lambda)$  is the absorbance at the Soret maxima of the free porphyrin and  $A(\lambda')$  is the corresponding absorbance of the bound form.

$$\%H = \frac{A(\lambda) - A(\lambda')}{A(\lambda)} \times 100 \quad (1)$$

For luminescence studies of Cu(TC3), the slit settings were 20 nm for excitation and emission. Normalizing the data using eq 2 facilitates

intensity comparisons by correcting for absorbance differences between samples.

$$I_{\text{norm}} = \frac{I_{\text{obs}}}{(1 - 10^{-A})} \quad (2)$$

In eq 2,  $I_{\text{norm}}$  is the adjusted intensity,  $I_{\text{obs}}$  is the observed emission intensity, and  $A$  is the absorbance at the exciting wavelength. Conversion of the CD signal from millidegrees into molar absorptivity units is possible with eq 3, where  $\theta$  is the observed value,  $Q = 32\,980$ ,  $l$  is the path length of the cell in centimeters, and  $c$  is the molar concentration of the chromophore.

$$\Delta\epsilon = \frac{\theta}{Qlc} \quad (3)$$

Sonicated ST DNA at a base-pair concentration of 70 μM was the host used for viscometry studies. The porphyrin stock solution was made in deionized water with no salt added. The monitoring temperature was 25 °C. Equation 4 gives the standard reduced viscosity ratio,

$$\frac{\eta}{\eta_0} = \frac{(t_c - t_b)}{(t_d - t_b)} \quad (4)$$

where  $t_b$  is the flow time of buffer,  $t_d$  is the flow time of DNA in buffer, and  $t_c$  is the flow time of DNA with porphyrin in buffer. The flow time was determined by taking the average of three consecutive runs for each composition.

**Crystallography.** A red needle of C<sub>48</sub>H<sub>58</sub>N<sub>12</sub>·4PF<sub>6</sub>·CH<sub>3</sub>CN having approximate dimensions of 0.22 × 0.14 × 0.10 mm was mounted on a fiber in a random orientation to determine the crystal structure. Preliminary examination and data collection were performed with Cu K $\alpha$  radiation ( $\lambda = 1.541\,84$  Å). Cell constants for data collection were obtained from least-squares refinement, using the setting angles of 70 136 reflections in the range of  $2 < \theta < 66^\circ$ . The space group was determined by the program XPREP.<sup>37</sup> The structure was solved by direct methods using SIR2004.<sup>38</sup> See Table 2 for crystal data and Figure 1 for a representation of the molecular structure of H<sub>2</sub>TC3, complete with an atom-numbering scheme.

**Instrumentation.** A Varian Cary 300 UV-vis spectrophotometer yielded absorbance data. Similarly emission data came from a Varian Cary Eclipse fluorescence spectrophotometer. Jasco J-810 and J-1500 spectropolarimeters yielded circular dichroism data. <sup>1</sup>H NMR data came from a 300 MHz Varian Mercury Inova spectrometer. A modified Cannon-Fenske model 25 viscometer yielded viscometric data, and the pH meter was a Corning model 430. Midwest Microlab,

**Table 2. Crystal Data and Data Collection Parameters for C<sub>48</sub>H<sub>58</sub>N<sub>12</sub>·4PF<sub>6</sub>·CH<sub>3</sub>CN**

formula	C <sub>50</sub> H <sub>61</sub> F <sub>24</sub> N <sub>13</sub> P <sub>4</sub>
formula weight	1423.99
space group	P $\bar{1}$ (No. 2)
$a$ , Å	12.1488(4)
$b$ , Å	14.8985(5)
$c$ , Å	19.1681(14)
$\alpha$ , deg	72.763(5)
$\beta$ , deg	71.762(5)
$\gamma$ , deg	70.043(5)
$V$ , Å <sup>3</sup>	3026.7(3)
$Z$	2
$d_{\text{calc}}$ , g cm <sup>-3</sup>	1.562
temperature, K	150
linear abs coef, mm <sup>-1</sup>	2.264
$2\theta$ range, deg	4.97–133.15
data collected	70 136
unique data	9558
$R(F_o)$	0.071
$R_w(F_o^2)$	0.201



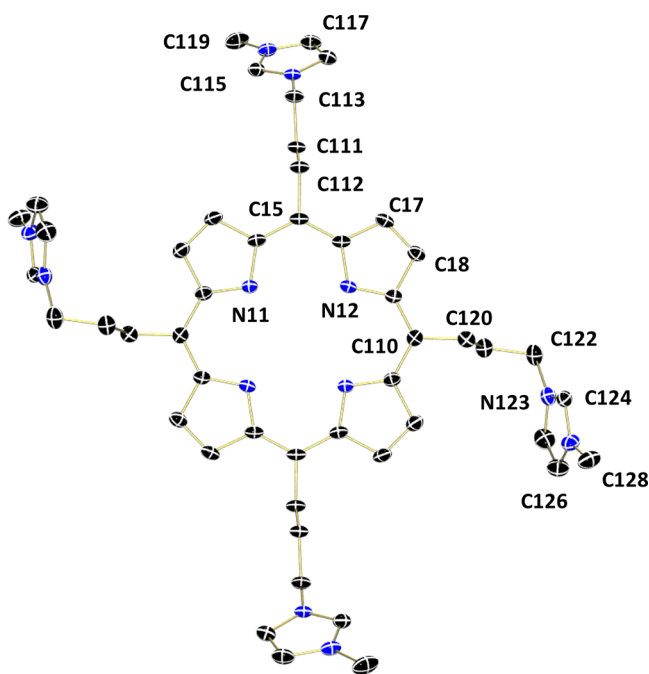


**Figure 1.** Representation of the cation in  $[\text{H}_2\text{TC3}](\text{PF}_6)_4 \cdot \text{CH}_3\text{CN}$  with thermal ellipsoids set at 50% probability. Hydrogen atoms omitted for clarity.

LLC (Indianapolis, IN) carried out all microanalyses. The diffractometer was Rigaku Rapid II equipped with confocal optics.

## RESULTS

**Characterization of Porphyrins.** Unlike the more rigid  $\text{H}_2\text{T4}$  analogue,  $\text{H}_2\text{TC3}$  is disadvantageously prone to aggregation in aqueous solution, as has been reported for tetra-substituted porphyrins with a pyridiniumyl ion extending off each alkyl chain.<sup>39</sup> In methanol, on the other hand, a Beer's law plot establishes that  $\text{H}_2\text{TC3}$  exists as a monomeric ion and exhibits a Soret maximum at 413 nm where  $\epsilon = 5.45 \times 10^5 \text{ M}^{-1} \text{ cm}^{-1}$ .  $\text{Cu}(\text{TC3})$  behaves similarly. It has a Soret maximum at 412 nm as well as a high molar absorptivity of  $6.0 \times 10^5 \text{ M}^{-1} \text{ cm}^{-1}$ . Figure 2 provides a contrast of the absorption spectra of

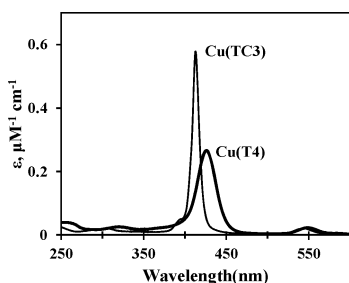


**Figure 2.** Absorbance spectra of  $\text{Cu}(\text{TC3})$  in methanol and  $\text{Cu}(\text{T4})$  in aqueous buffer.

$\text{Cu}(\text{TC3})$  and  $\text{Cu}(\text{T4})$ . The broadened bandwidth of the latter presumably relates to the pyridiniumyl substituents, which can assume a distribution of torsion angles. The same effect is sometimes evident in the emission spectrum of  $\text{H}_2\text{T4}$ , albeit in the Q-band region of the electronic spectrum.<sup>40</sup> In terms of emission neither  $\text{Cu}(\text{T4})$  nor  $\text{Cu}(\text{TC3})$  exhibits a detectable signal in methanol or methanol/water mixtures.

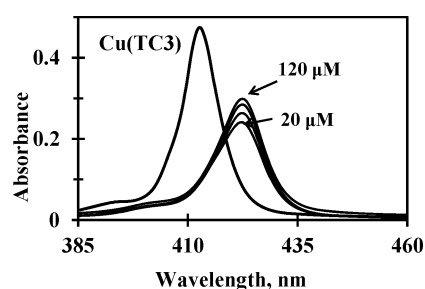
**DNA Titrations with  $\text{Cu}(\text{TC3})$ .** Absorbance measurements clearly signal that  $\text{Cu}(\text{TC3})$  readily binds to DNA hosts in aqueous solution. Moreover, data compiled in Table 3 show that the base composition of the host makes little difference. Illustrative results obtained with the hairpin host GATTAC appear in Figure 3; they reveal that interaction with the host induces a significant hypochromic shift as well as a strong bathochromic response in the Soret band. Here, the progression of the absorbance changes indicates that the chromophore actually experiences a succession of binding environments during the titration.<sup>41</sup> In particular, the hypochromic response is strongest in the early stages, prior to attainment of the limiting spectrum, which settles in with a bathochromic shift of  $\Delta\lambda = 10 \text{ nm}$  and a hypochromic response of  $H = 38\%$  (Table 3). Band shifts of those magnitudes are usually indicative of intercalative binding to ds DNA, both effects resulting from coupling of porphyrin absorption with electronic transitions of DNA bases.<sup>42</sup> Corresponding changes in the DNA absorbance ought to be present as well, but they are usually harder to observe on account of the density of states in the UV region of the spectrum.<sup>43</sup> When the DNA takes up  $\text{Cu}(\text{TC3})$ , however, a hyperchromic effect is clearly evident in the 260 nm region of the spectrum (Figure 4). (A referee points out, however, that the weak porphyrin absorbance in this region of the spectrum, evident in Figure 2, could also be a factor.) Reliable estimation of binding constants is problematic because of the poor solubility of the free porphyrin and the cooperative interactions between bound chromophores.<sup>20,41</sup> However, the titration results in Figure 3 suggest that the uptake of  $\text{Cu}(\text{TC3})$  by DNA is roughly as facile as that of  $\text{Cu}(\text{T4})$ . By that reckoning, the dissociation constant  $K_d$  would be on the order of  $10^{-6} \text{ M}$  with DNA in units of base pairs.<sup>44</sup>

The binding interactions manifest themselves in other physical studies as well. The observation of luminescence from  $\text{Cu}(\text{TC3})$  is particularly telling because the free porphyrin is essentially nonemissive in solution, while a relatively strong emission signal is a clear indication of intercalative binding (Figure 5).<sup>2,18,20,29</sup> For perspective, note that  $\text{Cu}(\text{T4})$  binds externally to the A=T-rich GATTAC host and is non-emitting,<sup>28</sup> whereas  $\text{Cu}(\text{TC3})$  is emissive because it binds by intercalation. Indeed, the signal obtained is 60% stronger than that produced by  $\text{Cu}(\text{T4})$  when it intercalates into GACGAC, which contains a higher percentage of G≡C base pairs. Along the same line, results in Table 3 show that the emission signal from  $\text{Cu}(\text{TC3})$  generally increases in intensity as the rigidity of the host and the percentage of G≡C base pairs increase. Adduct formation with a host like GATTAC also brings about an iCD signal from otherwise CD-silent  $\text{Cu}(\text{TC3})$ . Although the iCD signals obtained are typically bisignate, the positive branch is comparatively weak and mostly occurs at shorter wavelengths (Table 3), as when GACGAC acts as host. When  $\text{Cu}(\text{TC3})$  binds to ST DNA, the iCD signal is also bisignate; however, the pattern inverts, and the negative branch shifts to the shorter wavelength side.

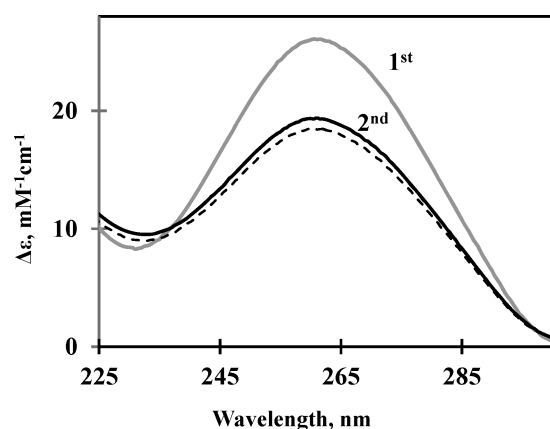
**DNA Titrations with  $\text{H}_2\text{TC3}$ .** There are obvious differences in the binding interactions of the unmetallated form of  $\text{H}_2\text{TC3}$ , despite the fact that it, too, is a nominally planar porphyrin. For G≡C-rich hosts like GACGAC, however, the spectral changes observed with  $\text{H}_2\text{TC3}$  mimic those of  $\text{Cu}(\text{TC3})$  in that the Soret band undergoes a large red shift, and the negative band of the iCD spectrum is dominant. On the other hand, as the host shifts to ST DNA and then GATTAC, the bathochromic shift in the limiting spectrum becomes progressively smaller (Figure

Table 3. Physical Data Obtained with ds Hosts

porphyrin	DNA host	absorbance		emission	iCD	
		$\Delta\lambda$ , nm	$H$ , %		$\lambda$ , nm	$\Delta\epsilon$ , M <sup>-1</sup> cm <sup>-1</sup>
Cu(TC3)	GACGAC	10	45	5.5	419	4
					427	-12
	GATTAC	10	38	5.5	419	7
					425	-15
	GCGCAC	10	43	7.8	424	-23
Zn(TC3)	AGCGCA	10	43	5.9	425	-14
	ST	10	35	4.2	422	-35
					430	8
	GACGAC	4	45		424	13
	GATTAC	2	40		425	6
H <sub>2</sub> TC3					432	-6
	ST	1	32		427	7
	GACGAC	9	43		416	16
					426	-27
	GATTAC	6	29		418	26
					425	-7
	GCGCAC	9	54		424	-35
	AGCGCA	9	39		425	-15
	ST	8	43		416	18
					426	-24



**Figure 3.** Absorption spectra of 1.0  $\mu\text{M}$  Cu(TC3) at  $q = 0$  and in the presence of the DNA hairpin GATTAC at  $q = 20, 40, 80$ , and  $120$ , respectively, which are the DNA concentrations in  $\mu\text{M}$  of base pairs. For the  $q = 0$  spectrum the solvent is methanol.



**Figure 4.** DNA absorbance changes during the addition of GATTAC to 1.0  $\mu\text{M}$  Cu(TC3). Each plot represents a 20  $\mu\text{M}$  aliquot of DNA and is the difference spectrum between two consecutive runs, those being  $q = 0$  and 20 (gray),  $q = 20$  and 40 (black), and  $q = 40$  and 60 (dashed). The hyperchromic effect recedes at higher  $q$  values because no porphyrin is available to interact with the added DNA.

6), and the positive branch of the iCD spectrum increases in importance. The Soret band also broadens, particularly when

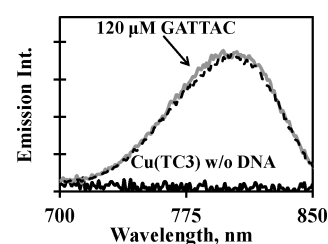


**Figure 5.** Absorbance-corrected emission spectra of Cu(TC3) in the absence of DNA (black) and in the presence of the DNA hairpin GATTAC at  $q = 20$  (dashed) and  $120$  (gray), which are the DNA concentrations in  $\mu\text{M}$  of base pairs. For the  $q = 0$  spectrum only the solvent is methanol.

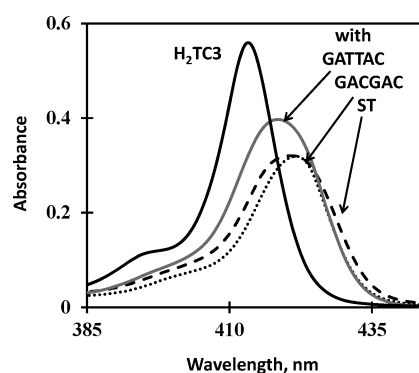


**Figure 6.** Absorption spectra of 1.0  $\mu\text{M}$  H<sub>2</sub>TC3 at  $q = 0$  (black) and in the presence of large excess of GATTAC (gray), ST (dashed), or GACGAC (dotted) DNA respectively. For the  $q = 0$  spectrum only the solvent is methanol.

ST DNA is the host. For this reason the  $H\%$  values reported in Table 3 sometimes exaggerate the actual hypochromic response, as the calculations ignore any change in band shape. (If one calculates the percent hypochromicity by comparing areas under the curves in Figure 6, the responses

are 3, 14, and 27 for the GATTAC, ST, and GACGAC hosts, respectively.)

**DNA Titrations with Zn(TC3).** Titrations reveal that the zinc-containing analogue Zn(TC3) binds to DNA as well. At least two stages of binding are evident in a titration with GACGAC. First, at a base-pair-to-Zn(TC3) ratio of  $q = 8$ , the Soret band exhibits sizable bathochromic and hypochromic responses (Figure 7). Addition of more host initially results in a

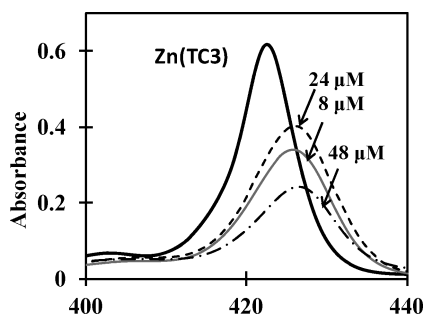


**Figure 7.** Absorption spectra of  $1.0 \mu\text{M}$  Zn(TC3) at  $q = 0$  (black) and in the presence of the DNA hairpin GACGAC at  $q = 8$  (gray), 24 (dashed), and 48 (dot dash), respectively. For the  $q = 0$  spectrum only the solvent is methanol.

weakening of the hypochromic effect, but in the presence of a large excess of DNA it strengthens once again, before leveling off at  $\sim q = 48$ . Figure 8 is an overlay of the iCD signals

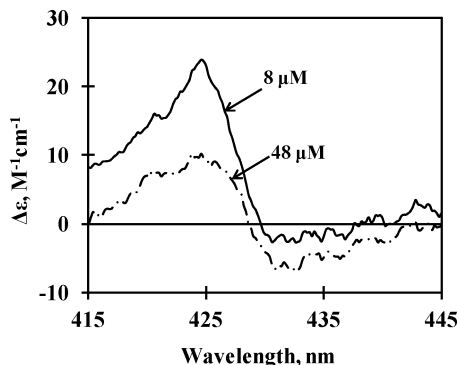


**Figure 8.** Induced CD spectra of  $1.0 \mu\text{M}$  Zn(TC3) when bound to the DNA hairpin GACGAC at DNA-to-porphyrin ratios of  $q = 8$  (line) and 48 (dot dash).

obtained at the two ends of the titration with GACGAC ( $q = 8$  and  $q = 48$ ). A titration with ST DNA reveals similar complexity. Thus, the hypochromic response steadily strengthens until  $q = 30$ , but the bathochromic shift sets in late, between  $q = 20$  and  $q = 50$ . At the  $q = 5$  stage there is no detectable iCD signal, but a weak positive signal is apparent at  $q = 50$  (Table 3). Compared with the results obtained with Cu(TC3), the bathochromic shifts and iCD signals, respectively, trend smaller and more positive with Zn(TC3), while the calculated  $H\%$  values tend to be larger. Again, however, binding to DNA tends to increase the width of the absorption band.

**Binding Studies with ss DNA.** Interactions with ss DNA hosts produce absorbance and emission spectra that in many ways parallel those described for ds DNA hosts. Thus, in the Soret region, Cu(TC3) once again exhibits the largest bathochromic shifts. When Cu(TC3) binds to the ss DNA host T<sub>10</sub>,  $\Delta\lambda = 8$  nm versus 10 nm with GATTAC, and the

hypochromic effect is actually a few percent larger with T<sub>10</sub> (Table 4). Interaction with T<sub>10</sub> also induces an emission signal

**Table 4.** Physical Data Obtained with ss Hosts

porphyrin	DNA host	absorbance		emission	iCD $\lambda, \text{nm}$	$\Delta\epsilon, \text{M}^{-1} \text{cm}^{-1}$
		$\Delta\lambda, \text{nm}$	$H, \%$			
Cu(TC3)	T <sub>10</sub>	8	33	3.8	421	21
	Puc	9	38	2.0	421	12
Zn(TC3)	T <sub>10</sub>	3	30		421	
	Puc	4	44		426	6
H <sub>2</sub> TC3	T <sub>10</sub>	5	33		431	3
	Puc	4	44		426	6

from Cu(TC3) that is  $\sim 70\%$  as intense as that obtained with GATTAC. With the purine-containing sequence Puc the bathochromic shift is a bit larger at 10 nm, but the emission signal is weaker by about a factor of 2. In the case of H<sub>2</sub>TC3 the bathochromic shifts are smaller than those observed for Cu(TC3), but the hypochromic responses are of comparable magnitudes. The smallest  $\Delta\lambda$  values result with Zn(TC3), but they are about equal in magnitude to those obtained with ds DNA hosts. In comparison with results obtained with ds DNA, the biggest departure occurs in the iCD signals. With the ss hosts the iCD signals are essentially monosignate and strictly positive for all three porphyrins. Cu(TC3) exhibits the most intense iCD signals and H<sub>2</sub>TC3 the weakest (Table 4).

**Viscometry and High-Concentration Solutions.** Viscometric data obtained for Cu(TC3) and Zn(TC3) are different. For these experiments the porphyrin concentrations are much higher than they are in the titration studies and range up to  $42 \mu\text{M}$ . Plots in Figure 9 show how the standard reduced viscosity

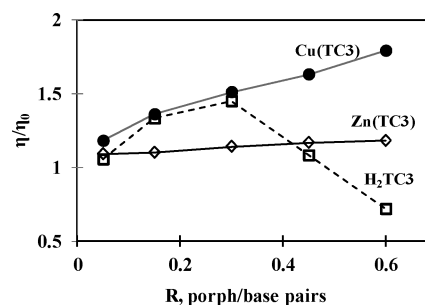


**Figure 9.** Standard viscosity ratios of ST DNA in the presence of Cu(TC3) (●), H<sub>2</sub>TC3 (□), and Zn(TC3) (◇). The DNA concentration remains constant at  $70 \mu\text{M}$  in base pairs, while the porphyrin-to-DNA pair ratio,  $R$ , varies. The buffer is  $\mu = 0.10 \text{ M}$  pH 7.5 Tris.

varies with the porphyrin-to-DNA base-pair ratio,  $R = q^{-1}$ , when Cu(TC3) or Zn(TC3) interacts with sonicated ST DNA in Tris buffer. The first thing to note is that the binding of Zn(TC3) has almost no measurable impact on the flow characteristics of the DNA host. In contrast,  $\eta/\eta_0$  nearly doubles with the uptake of Cu(TC3) as  $R$  ranges from 0.1–0.6. Specific viscosity increases of that magnitude are generally an indication of intercalative binding, which induces an increase in length as well as a decrease in flexibility of the macromolecular host.<sup>17</sup> At the same time absorbance studies reveal that Cu(TC3) adopts a second binding motif in this same concentration regime. Whereas Cu(TC3) normally exhibits a single, red-shifted Soret band, a second Soret maximum appears

at the higher  $R$  values, and it is indicative of a separate bound form (Figure 10). Likewise, the CD spectrum shows a band in

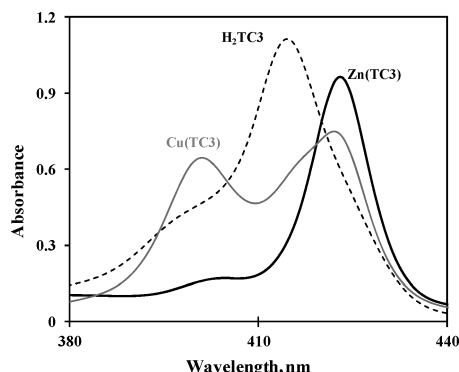


**Figure 10.** Absorbance spectra of Cu(TC3) (gray), H<sub>2</sub>TC3 (dashed), and Zn(TC3) (black), in the presence of ST DNA. In each case the DNA base-pair concentration is 30  $\mu$ M, and the porphyrin concentration is 10  $\mu$ M. Cell path length is 2.0 mm.

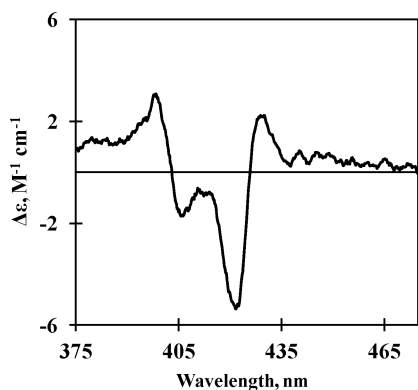


**Figure 11.** Induced CD spectrum of 10.0  $\mu$ M Cu(TC3) when bound to ST DNA at a DNA base-pair concentration of 30.0  $\mu$ M. Cell path length is 2.0 mm.

the vicinity of 400 nm (Figure 11). Emission data obtained at  $R = 0.3$  confirm the existence of the second binding motif because the 400 nm transition does *not* appear in the excitation spectrum of Cu(TC3). By  $R = 0.5$  the 400 nm absorption maximum is dominant, and the overall pattern of absorbance broadens. A 400 nm band maximum also appears in spectra of simple aqueous salt solutions containing like porphyrins. Excitonic coupling interactions have been posited to account for the shift of the Soret band to shorter wavelength due to formation of H-type, face-to-face porphyrin aggregates.<sup>39</sup> In contrast, there is no evidence of a hypsochromically shifted absorption for Zn(TC3) in the same concentration regime. The probable explanation is that zinc(II) porphyrins show a preference for binding axial ligands,<sup>3,45</sup> which interfere with stacking interactions.

Finally, the H<sub>2</sub>TC3 system represents a third variation. Figure 9 reveals that the specific viscosity of ST DNA initially increases with the addition of H<sub>2</sub>TC3, as with Cu(TC3). However, beyond  $R = 0.3$ ,  $\eta/\eta_0$  begins to fall off, and by  $R = 0.5$  the specific viscosity drops below that observed for the free DNA. In terms of absorbance, a distinct broadening of the spectrum is evident when the ST concentration is 30  $\mu$ M and

the porphyrin concentration is 15  $\mu$ M. New absorbance also grows in the vicinity of 400 nm; however, it is in the form of a poorly resolved shoulder, rather than the clearly resolved maximum obtained with Cu(TC3).

## DISCUSSION

**Ligand Design and Choice of Hosts.** Incorporating alkyl substituents in the meso positions of the porphyrin achieves at least three ends. One is to isolate the  $\pi$  system of the porphyrin and avoid the mesomeric interactions that typically occur with aryl substituents. The upshot is a narrower bandwidth and a higher molar absorptivity for the Soret absorption of H<sub>2</sub>TC3 as compared with H<sub>2</sub>T4. While alkyl substituents clearly contribute to the bulkiness,<sup>24</sup> the flexible nature of the chains makes for a sterically more accommodating system than H<sub>2</sub>T4. Finally, the four peripheral charges no longer have to extend outward in a fixed plane, as is the case with H<sub>2</sub>T4. An unintended result of the design is that H<sub>2</sub>TC3 is subject to self-association in aqueous salt solutions. The same complication does not occur with the H<sub>2</sub>T4 system,<sup>46</sup> perhaps because of the bulkiness and immobility of the meso substituents.

In terms of hosts, hairpin-forming sequences most often bind ligands in the double-helical stem domains; hence, they are viable B-form DNA platforms.<sup>20,47,48</sup> In addition to being cost-effective, they offer a defined length and a programmable base composition. Including the interior sequence 5'-CttttG-3' provides for a tight loop and thermodynamic stability.<sup>47,49</sup> Sonicated ST DNA serves as a useful contrast, effectively functioning as a random sequence DNA polymer compatible with viscometric studies. Finally, single-stranded DNA hosts provide interesting comparisons because they are relatively flexible, and the exposed face is more hydrophobic than is the case with a ds DNA host.<sup>50</sup> Like the latter, ss hosts are capable of binding ligands externally or internally. The term often used to describe internal binding is pseudointercalation, which involves sandwiching the ligand between adjacent bases of the host.<sup>51,52</sup> The lengths of T<sub>10</sub> and Puc reflect the fact that exposed runs of naturally occurring ss DNA are generally short.<sup>53</sup> Finally, the host compositions are complementary in that T<sub>10</sub> contains a single repeating pyrimidine base, while Puc has mixed composition including both adenine and guanine bases.

**Preferential Internalization of Cu(TC3).** The results of all of the physical studies establish that Cu(TC3) preferentially internalizes into DNA hosts. In the first place, intercalative binding naturally explains the observed bathochromic and hypochromic responses, which are explicable in terms of excitonic coupling interactions with  $\pi-\pi^*$  transitions of the DNA bases.<sup>12,42</sup> Second, that kind of internalization is necessary to account for the observation of an emission signal; otherwise, associative attack by Lewis bases efficiently quenches the photoexcited state.<sup>18,20,26,54</sup> Finally, the fact that the uptake of Cu(TC3) induces an increase in the specific viscosity of ST DNA represents classical evidence of intercalative binding.<sup>17</sup> The uniformity of the absorption and emission results indicate that the mode of binding does not depend on the base makeup of the host because the percentage of G $\equiv$ C base pairs varies by a factor of 2 across ST DNA and the stem domains of GATTAC and GACGAC. In contrast, Cu[T4] is only capable of intercalating into only high-melting duplexes that contain at least 50% G $\equiv$ C base pairs.<sup>55</sup> At lower percentages local melting of the duplex structure becomes more feasible, and external binding of Cu(T4) becomes more favorable. The



problem posed by intercalation derives from steric clashes that occur between the pyridiniumyl substituents of the porphyrin and the sugar–phosphate backbone of the host.<sup>16</sup> Cu(TC3) is more compatible with intercalative binding because it has more flexible substituents. The story is similar to ss DNA hosts, which bind Cu(TC3) strictly by pseudointercalation. As before, the evidence for assigning the binding motif comes from the strong hypochromic shifts and emission signals generated by uptake. Internalization of Cu(TC3) by T<sub>10</sub> is so effective in that the emission intensity rivals that observed from Cu(T4) intercalated into GACGAC.

At intermediate loadings ( $q = 8\text{--}16$ ), another effect comes into play, as Figure 3 reveals that the hypochromic effect is higher in the initial stages of a titration. This effect is readily understandable in terms of dipole–dipole coupling between the transition moments of neighboring, intercalatively bound porphyrins.<sup>41</sup> This observation suggests that uptake may be somewhat cooperative because there are more host molecules than porphyrins in solution. In view of the absorption strength of Cu(TC3), the separation between bound chromophores could easily be as much as a few base pairs, however.<sup>56,57</sup> At higher overall concentration the binding picture becomes even more complex. Indeed, as noted above, results obtained with ST DNA show that another type of cooperative association occurs as Cu(TC3) begins to aggregate in H-type fashion on the surface of the host. The signature for that binding motif is the Soret band, which starts to grow in at 400 nm, beyond the normal red-shifted band found in the vicinity of 420 nm (Figure 10). That the H-form porphyrin is a DNA-bound form follows from the fact that the 400 nm transition also shows an induced CD signal. It is, however, a separate fraction of porphyrin because the 400 nm band is absent in the emission excitation spectrum.

**External Binding of Zn(TC3) and H<sub>2</sub>TC3.** The most definitive information about the binding of Zn(TC3) comes from viscometric data, which show that it does not intercalate into ST DNA. It therefore must bind externally. Because the viscometry data relate to relatively high-loading conditions, the discussion that follows strictly pertains to the early phases of titrations, in the  $q = 8\text{--}16$  region; however, there are no indications of a qualitative change in the mode of binding when the DNA is in large excess. For all the ds hosts, including ST DNA, the small bathochromic shifts ( $\Delta\lambda$  values) are consistent with external binding. For the sake of reference,  $\Delta\lambda = 2$  nm when Zn(T4) binds externally to [poly(dA–dT)]<sub>2</sub>, whereas the shift is 6 times greater when Zn(tD4) intercalates into the same host.<sup>25</sup> The iCD data also imply that the zinc and copper forms of the porphyrin bind very differently to DNA. In contrast to the results obtained with Cu(TC3), the interaction of Zn(TC3) with ds DNA produces iCD signals that are biphasic, but predominantly *positive*. The most curious finding is that external binding of Zn(TC3) produces such strong hypochromic responses, although it is important to note that binding to DNA dramatically enhances the width of the Soret absorption band. Heterogeneity may partly explain the broadening effect if there is no one preferred binding sequence or adduct structure. Distortion of the porphyrin is another possibility, *vide infra*. The most likely explanation for the change of binding motif is that, in contrast to copper(II) analogues, zinc(II) porphyrins prefer to bind an axial ligand.<sup>3</sup> Intercalation of a Zn(II) porphyrin would still be possible if the process were exothermic enough to compensate for the loss of

the bond to the axial ligand;<sup>20</sup> however, that is obviously not the case with Zn(TC3).

In contrast, H<sub>2</sub>TC3 is capable of intercalating because the standard reduced viscosity of ST DNA increases with the addition of H<sub>2</sub>TC3 up to a value of  $R = 0.3$ . The  $\eta/\eta_0$  values are slightly smaller than those observed with Cu(TC3), because external binding of H<sub>2</sub>TC3 is a competitive process. That there are two binding motifs becomes clear from a comparison of results obtained with the three hosts GATTAC, ST, and GACGAC, which have percentage compositions of G≡C base pairs of 33, 41, and 66, respectively. The spectra presented in Figure 6 show that the bathochromic shift  $\Delta\lambda$  increases steadily as the percentage of G≡C pairs increases. The GACGAC system is the simplest because of its relatively high G≡C content. Here, the bathochromic shift is large, intercalative binding is dominant, and the Soret band has a normal bandwidth. With ST DNA,  $\Delta\lambda$  is smaller, and external binding becomes more important because the host contains a higher percentage of A=T base pairs. The presence of two active modes of binding accounts for the increase in the apparent bandwidth because in reality the signal is the envelope of two unresolved absorptions. Finally, when GATTAC is the host, external binding becomes even more important, and the net bathochromic shift is smaller. As for the iCD data, the overall signal becomes on the whole more negative as the percentage of G≡C base pairs increases. This trend is also indicative of an increase in the fraction of intercalated porphyrin.

**Mutually Adaptive Distortions.** The problem that remains is to understand why H<sub>2</sub>TC3 and Cu(TC3) bind differently to ds DNA. The zinc(II) system stands apart, of course, because it carries an axial ligand. The issue is that Cu(TC3) binds as an intercalator, while external binding is much more important for H<sub>2</sub>TC3 even though both porphyrins are nominally planar ligands. The rigidity of the host is clearly a decisive factor because the intercalation of H<sub>2</sub>TC3 becomes more important as the G≡C content increases. Hence it is logical to infer that the rigidity of the porphyrin has an influence as well. In particular, H<sub>2</sub>TC3 is amenable to undergoing an out-of-plane distortion, whereas studies have established that relatively large metal ions like Cu(II) fill the porphyrin cavity and reinforce planarity. Experimental evidence for the latter conclusion comes from studies of the rates of racemization of planar chiral porphyrins,<sup>58</sup> as well as kinetic studies of atropisomerization processes.<sup>59,60</sup> To see why distortion of the porphyrin might influence the mode of binding, it is helpful to consider how ligand binding affects the structure of the DNA host.

The first thing to note is that high-affinity binding of a cationic porphyrin to DNA necessarily involves an induced fit. For example, for a porphyrin to intercalate, the DNA host has to unwind and create a cavity to house the ligand.<sup>61</sup> In favorable circumstances the host maintains base pairing and its double-helical structure; however, the uptake of a very bulky ligand may disrupt Watson–Crick base pairing, at the same time forcing a base to extend or “flip” out into the solution environment.<sup>16,62</sup> In contrast, the host structure or structures that support high-affinity external binding in solution remain to be identified. Solid-state structures of externally bound porphyrins are available,<sup>11,63</sup> but the relevance to solution work is unclear because the porphyrin sandwiches between neighboring hosts in the crystal lattice. A complicating factor is that porphyrins are not natural groove binders because they do not have the crescent shape of netropsin.<sup>64</sup> Accordingly, many

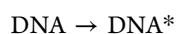


investigators agree that the DNA molecule almost certainly has to distort from its canonical structure and form a suitable binding pocket to bind a bulky porphyrin ligand with high affinity.<sup>20,31,65,66</sup> Formation of the pocket presumably involves generating a suitable hydrophobic surface while at the same time promoting Coulombic contacts. From that point of view the term “external binding” may be a bit of a misnomer; indeed, recent quenching studies of externally bound Pd(T4) suggest that the host largely envelops the ligand.<sup>29</sup>

A sympathetic or compensatory distortion of the porphyrin ligand could certainly bolster the interaction with a reorganized host, and the most likely motion within the core is an out-of-plane distortion.<sup>67,68</sup> The impetus for the distortion can come from internal forces, such as cadmium(II) insertion (induces doming) or protonation of core nitrogens (results in saddling).<sup>67,69</sup> Alternatively, incorporating bulky alkyl or aryl substituents on the periphery of the porphyrin can also lead to saddling.<sup>67</sup> Host–guest interactions are another possibility. Thus, Yatsunyk and co-workers have published an X-ray structure that suggests the domed structure of *N*-methyl mesoporphyrin IX predisposes it to bind to human telomeric G-Quadruplex DNA because the 3'-G-tetrad of the host naturally presents a complementary inverted domelike surface geometry.<sup>70</sup> In addition, they propose that additional distortions in the host and guest mutually reinforce each other in the course of adduct formation. Host–guest interactions similarly influence the binding of H<sub>2</sub>TC3. When H<sub>2</sub>TC3 binds to a flexible DNA host like T<sub>10</sub>, the half width of the Soret band increases noticeably, consistent with induction of a distortion.<sup>71</sup> In contrast, incorporating copper(II) stiffens the porphyrin, and the half width of the Soret band of a DNA-bound form generally remains narrow. It is worth noting that the H<sub>2</sub>T4 system is also relatively inflexible in that its aryl substituents constrain the positive charges to extend outward. That may explain why H<sub>2</sub>T4 exclusively intercalates into the G≡C-rich host GACGAC, while external binding remains a competitive process for the more fluid H<sub>2</sub>TC3 porphyrin.

## VISTA

The striking finding that Cu(TC3) intercalates into the A=T-rich host GATTAC, while H<sub>2</sub>TC3 binds externally, is an indication that a number of forces jointly influence the binding motif.<sup>20</sup> Studies involving Cu(T4) and the 5'-GAA-GACT<sub>4</sub>GTCTTC-3' hairpin illustrate the impact the base composition has.<sup>19</sup> Whereas Cu(T4) intercalates into the hairpin, the same porphyrin shifts to external binding when base replacement results in the loss of even one hydrogen bond in the stem. Fortunately, the above results find a simple explanation in the context of a simple two-step thermodynamic model.<sup>20</sup> Step one takes account of the structural reorganization required of the DNA host along with the associated free energy change  $\Delta G_R$ . Step two incorporates the binding energy released ( $\Delta G_B$ ) upon adduct formation with the preorganized host (DNA\*).



The elementary version of the model being invoked assumes any reorganization energy associated with the porphyrin is small, although at a minimum desolvation must occur. As one application, recall that Cu(T4) intercalates into the GACGAC hairpin but binds externally to GATTAC.<sup>20,28</sup> In the context of

the model, the GACGAC host is relatively rich in G≡C base pairs and not very compatible with external binding due to a high  $\Delta G_R$  barrier. In contrast, external binding becomes the preferred motif with the GATTAC host due to fewer hydrogen bonds in the stem, a lower melting temperature, and a reduced  $\Delta G_R$  barrier. The Cu(TC3) ligand, on the other hand, preferentially intercalates into the GATTAC host, presumably because of reduced strain in the minor groove domain and a more favorable  $\Delta G_B$  term. The bigger challenge is understanding why the unmetallated porphyrin H<sub>2</sub>TC3 preferentially binds *externally*. Most likely, H<sub>2</sub>TC3 is uniquely capable of undergoing a sympathetic distortion that enhances the induced fit ( $\Delta G_B$  term). As Cu(TC3) and H<sub>2</sub>TC3 carry identical substituents, in all likelihood the distortion involves a core rearrangement, that is, an out-of-plane distortion. The possibility of a propeller distortion is particularly intriguing in this regard because it would render the porphyrin intrinsically chiral and directly impact the iCD signal.<sup>72,73</sup>

The above results illustrate that ligand modification is an effective strategy for tuning the reactivities of metal-containing complexes with biomolecules. Further options to explore with M(TC3) systems include terminating the alkyl substituents with amine groups so that introducing charge is possible by protonation or conjugation with therapeutically active metal ions.<sup>74</sup> Shortening the chain length is also possible and could encourage dissolution as a monomer in water. In closing it is worth noting that ligand modification is equally profitable as a tuning strategy when the metal complex has a nonplanar coordination geometry. To cite a few examples, Barton and co-workers have studied ruthenium(II) polypyridine complexes and have shown that elongating one of the conjugated ligands promotes intercalative binding.<sup>75</sup> The same group has also shown that introducing an oversized ligand destabilizes intercalative binding in favor of insertion at sites where there is a base-pair mismatch.<sup>76</sup> Working with the same metal center, Glazer and co-workers have shown that introducing a bulky ligand induces light-activatable anticancer activity.<sup>77</sup> Finally, utilizing dirhodium frameworks, Dunbar and Turro have shown that varying the number of coordinated polypyridines can affect the binding motif,<sup>78</sup> while the aspect ratio of the active ligand impacts the mode of uptake as well as the binding affinity.<sup>79</sup>

## ASSOCIATED CONTENT

### Supporting Information

CIF file showing crystallographic data and structural information. This material is available free of charge via the Internet at <http://pubs.acs.org>.

## AUTHOR INFORMATION

### Corresponding Author

\*E-mail: [mcmillin@purdue.edu](mailto:mcmillin@purdue.edu).

### Notes

The authors declare no competing financial interest.

## ACKNOWLEDGMENTS

The NSF funded this research via Grant Nos. CHE 0847229 and CBET-11097833.

## REFERENCES

- (1) Fiel, R. J. *J. Biomol. Struct. Dyn.* **1989**, 6, 1259–1275.
- (2) McMillin, D. R.; McNett, K. M. *Chem. Rev.* **1998**, 98, 1201–1219.

- (3) Pasternack, R. F.; Gibbs, E. J.; Villafranca, J. J. *Biochemistry* **1983**, *22*, 2406–2414.
- (4) Snyder, J. W.; Lambert, J. D. C.; Ogilby, P. R. *Photochem. Photobiol.* **2006**, *82*, 177–184.
- (5) Tada-Oikawa, S.; Oikawa, S.; Hirayama, J.; Hirakawa, K.; Kawanishi, S. *Photochem. Photobiol.* **2009**, *85*, 1391–1399.
- (6) Milgrom, L.; MacRobert, S. *Chem. Ber.* **1998**, *34*, 45–50.
- (7) MacDonald, I. J.; Dougherty, T. J. *J. Porphyrins Phthalocyanines* **2001**, *5*, 105–129.
- (8) Agostinis, P.; Berg, K.; Cengel, K. A.; Foster, T. H.; Girotti, A. W.; Gollnick, S. O.; Hahn, S. M.; Hamblin, M. R.; Juzeniene, A.; Kessel, D.; Korbelik, M.; Moan, J.; Mroz, P.; Nowis, D.; Piette, J.; Wilson, B. C.; Golab, J. *Ca—Cancer J. Clin.* **2011**, *61*, 250–281.
- (9) Hamblin, M. R.; O'Donnell, D. A.; Murthy, N.; Contag, C. H.; Hasan, T. *Photochem. Photobiol.* **2002**, *75*, 51–57.
- (10) Han, F. X. G.; Wheelhouse, R. T.; Hurley, L. H. *J. Am. Chem. Soc.* **1999**, *121*, 3561–3570.
- (11) Parkinson, G. N.; Ghosh, R.; Neidle, S. *Biochemistry* **2007**, *46*, 2390–2397.
- (12) Biver, T. *Appl. Spectrosc. Rev.* **2012**, *47*, 272–325.
- (13) Mukundan, N. E.; Petho, G.; Dixon, D. W.; Marzilli, L. G. *Inorg. Chem.* **1995**, *34*, 3677–3687.
- (14) Marzilli, L. G.; Petho, G.; Lin, M. F.; Kim, M. S.; Dixon, D. W. *J. Am. Chem. Soc.* **1992**, *114*, 7575–7577.
- (15) Pasternack, R. F. *Chirality* **2003**, *15*, 329–332.
- (16) Lipscomb, L. A.; Zhou, F. X.; Presnell, S. R.; Woo, R. J.; Peek, M. E.; Plaskon, R. R.; Williams, L. D. *Biochemistry* **1996**, *35*, 2818–2823.
- (17) Strickland, J. A.; Marzilli, L. G.; Gay, K. M.; Wilson, W. D. *Biochemistry* **1988**, *27*, 8870–8878.
- (18) Hudson, B. P.; Sou, J.; Berger, D. J.; McMillin, D. R. *J. Am. Chem. Soc.* **1992**, *114*, 8997–9002.
- (19) Tears, D. K. C.; McMillin, D. R. *Chem. Commun. (Cambridge, U.K.)* **1998**, 2517–2518.
- (20) McMillin, D. R.; Shelton, A. H.; Bejune, S. A.; Fanwick, P. E.; Wall, R. K. *Coord. Chem. Rev.* **2005**, *249*, 1451–1459.
- (21) Sari, M. A.; Battioni, J. P.; Mansuy, D.; Lepecq, J. B. *Biochem. Biophys. Res. Commun.* **1986**, *141*, 643–649.
- (22) Manono, J.; Marzilli, P. A.; Fronczek, F. R.; Marzilli, L. G. *Inorg. Chem.* **2009**, *48*, 5626–5635.
- (23) Fiel, R. J.; Howard, J. C.; Mark, E. H.; Dattagupta, N. *Nucleic Acids Res.* **1979**, *6*, 3093–3118.
- (24) Andrews, K.; McMillin, D. R. *Biochemistry* **2008**, *47*, 1117–1125.
- (25) Wall, R. K.; Shelton, A. H.; Bonaccorsi, L. C.; Bejune, S. A.; Dube, D.; McMillin, D. R. *J. Am. Chem. Soc.* **2001**, *123*, 11480–11481.
- (26) Bejune, S. A.; Shelton, A. H.; McMillin, D. R. *Inorg. Chem.* **2003**, *42*, 8465–8475.
- (27) Wu, S.; Li, Z.; Ren, L. G.; Chen, B.; Liang, F.; Zhou, X.; Jia, T.; Cao, X. P. *Bioorg. Med. Chem.* **2006**, *14*, 2956–2965.
- (28) Briggs, B. N.; Gaier, A. J.; Fanwick, P. E.; Dogutan, D. K.; McMillin, D. R. *Biochemistry* **2012**, *51*, 7496–7505.
- (29) Bork, M. A.; Gianopoulos, C. G.; Zhang, H.; Fanwick, P. E.; Choi, J. H.; McMillin, D. R. *Biochemistry* **2014**, *53*, 714–724.
- (30) Corey, E. J.; Suggs, J. W. *Tetrahedron Lett.* **1975**, 2647–2650.
- (31) Fiel, R. J.; Jenkins, B. G.; Alderfer, J. L. In *Molecular Basis of Specificity in Nucleic-Acid-Drug Interactions*; Pullman, B., Jortner, J., Eds.; Kluwer Academic: Dordrecht, The Netherlands, 1990; pp 385–399.
- (32) Kadish, K. M.; Ou, Z. P.; Zhan, R. Q.; Khoury, T.; Wenbo, E.; Crossley, M. J. *J. Porphyrins Phthalocyanines* **2010**, *14*, 866–876.
- (33) Wu, X. E.; Ma, L.; Ding, M. X.; Gao, L. X. *Chem. Lett.* **2005**, *34*, 312–313.
- (34) Batinic-Haberle, I.; Spasojevic, I.; Hambright, P.; Benov, L.; Crumbliss, A. L.; Fridovich, I. *Inorg. Chem.* **1999**, *38*, 4011–4022.
- (35) Sambrook, J.; Fritsch, E. F.; Maniatis, T. *Molecular Cloning a Laboratory Manual*, 2nd ed.; Cold Spring Harbor Press: Cold Spring Harbor, NY, 1989; Vol 3.
- (36) Felsenfeld, G.; Hirschman, S. Z. *J. Mol. Biol.* **1965**, *13*, 407–427.
- (37) Sheldrick, G. M. *Acta Crystallogr., Sect. A* **2008**, *64*, 112–122.
- (38) Burla, M. C.; Caliendo, R.; Camalli, M.; Carrozzini, B.; Cascarano, G. L.; De Caro, L.; Giacovazzo, C.; Polidori, G.; Spagna, R. *J. Appl. Crystallogr.* **2005**, *38*, 381–388.
- (39) Kano, K.; Fukuda, K.; Wakami, H.; Nishiyabu, R.; Pasternack, R. F. *J. Am. Chem. Soc.* **2000**, *122*, 7494–7502.
- (40) Vergeldt, F. J.; Koehorst, R. B. M.; Vanhoek, A.; Schaafsma, T. J. *J. Phys. Chem.* **1995**, *99*, 4397–4405.
- (41) Shelton, A. H.; Rodger, A.; McMillin, D. R. *Biochemistry* **2007**, *46*, 9143–9154.
- (42) von Holde, K. E.; Johnson, W. C.; Pui, S. H. *Principles of Physical Biochemistry*, 2nd ed.; Prentice Hall: Upper Saddle River, NJ, 2006.
- (43) Cantor, C. R.; Schimmel, P. R. *Biophysical Chemistry*, Freeman: San Francisco, CA, 1980; Vol. 2, Ch. 7.
- (44) Strickland, J. A.; Marzilli, L. G.; Wilson, W. D. *Biopolymers* **1990**, *29*, 1307–1323.
- (45) Collins, D. M.; Hoard, J. L. *J. Am. Chem. Soc.* **1970**, *92*, 3761–&.
- (46) Ito, A. S.; Azzellini, G. C.; Silva, S. C.; Serra, O.; Szabo, A. G. *Biophys. Chem.* **1992**, *45*, 79–89.
- (47) Lugo-Ponce, P.; McMillin, D. R. *Coord. Chem. Rev.* **2000**, *208*, 169–191.
- (48) Rentzeperis, D.; Alessi, K.; Marky, L. A. *Nucleic Acids Res.* **1993**, *21*, 2683–2689.
- (49) Antao, V. P.; Lai, S. Y.; Tinoco, I. *Nucleic Acids Res.* **1991**, *19*, 5901–5905.
- (50) Jain, R. K.; Sarracino, D. A.; Richert, C. *Chem. Commun. (Cambridge, U.K.)* **1998**, 423–424.
- (51) Pasternack, R. F.; Brigandi, R. A.; Abrams, M. J.; Williams, A. P.; Gibbs, E. J. *Inorg. Chem.* **1990**, *29*, 4483–4486.
- (52) Biancardi, A.; Biver, T.; Marini, A.; Mennucci, B.; Secco, F. *Phys. Chem. Chem. Phys.* **2011**, *13*, 12595–12602.
- (53) Wadkins, R. M. *Curr. Med. Chem.* **2000**, *7*, 1–15.
- (54) Chirvony, V. S. *J. Porphyrins Phthalocyanines* **2003**, *7*, 766–774.
- (55) Eggleston, M. K.; Crites, D. K.; McMillin, D. R. *J. Phys. Chem. A* **1998**, *102*, 5506–5511.
- (56) Lewis, F. D.; Zhang, L. G.; Liu, X. Y.; Zuo, X. B.; Tiede, D. M.; Long, H.; Schatz, G. C. *J. Am. Chem. Soc.* **2005**, *127*, 14445–14453.
- (57) Lewis, F. D. *Photochem. Photobiol.* **2005**, *81*, 65–72.
- (58) Konishi, K.; Miyazaki, K.; Aida, T.; Inoue, S. *J. Am. Chem. Soc.* **1990**, *112*, 5639–5640.
- (59) Gottwald, L. K.; Ullman, E. F. *Tetrahedron Lett.* **1969**, 3071–&.
- (60) Freitag, R. A.; Whitten, D. G. *J. Phys. Chem.* **1983**, *87*, 3918–3925.
- (61) Calladine, C. R.; Drew, H. R. *Understanding DNA*; Academic: New York, 1997.
- (62) Norden, B.; Lincoln, P.; Akerman, B.; Tuite, E. Probing of Nucleic Acids by Metal Ion Complexes of Small Molecules. In *Metal Ions in Biological Systems*; Sigel, A., Sigel, H., Eds.; CRC Press: Boca Raton, FL, 1996; Vol. 33, pp 177–252.
- (63) Bennett, M.; Krah, A.; Wien, F.; Garman, E.; McKenna, R.; Sanderson, M.; Neidle, S. *Proc. Natl. Acad. Sci. U. S. A.* **2000**, *97*, 9476–9481.
- (64) Neidle, S. *Nat. Prod. Rep.* **2001**, *18*, 291–309.
- (65) Gibbs, E. J.; Maurer, M. C.; Zhang, J. H.; Reiff, W. M.; Hill, D. T.; Malickablaszkiewicz, M.; McKinnie, R. E.; Liu, H. Q.; Pasternack, R. F. *J. Inorg. Biochem.* **1988**, *32*, 39–65.
- (66) Sehlstedt, U.; Kim, S. K.; Carter, P.; Goodisman, J.; Vollano, J. F.; Norden, B.; Dabrowiak, J. C. *Biochemistry* **1994**, *33*, 417–426.
- (67) Sparks, L. D.; Medforth, C. J.; Park, M. S.; Chamberlain, J. R.; Ondrias, M. R.; Senge, M. O.; Smith, K. M.; Shelnutt, J. A. *J. Am. Chem. Soc.* **1993**, *115*, 581–592.
- (68) Senge, M. O. *Chem. Commun. (Cambridge, U.K.)* **2006**, 243–256.
- (69) Cheng, B. S.; Munro, O. Q.; Marques, H. M.; Scheidt, W. R. *J. Am. Chem. Soc.* **1997**, *119*, 10732–10742.
- (70) Nicoludis, J. M.; Miller, S. T.; Jeffrey, P. D.; Barrett, S. P.; Rablen, P. R.; Lawton, T. J.; Yatsunyk, L. A. *J. Am. Chem. Soc.* **2012**, *134*, 20446–20456.

- (71) D'Souza, F.; Villard, A.; Vancaemelbecke, E.; Franzen, M.; Boschi, T.; Tagliatesta, P.; Kadish, K. M. *Inorg. Chem.* **1993**, *32*, 4042–4048.
- (72) Shelnutt, J. A.; Song, X. Z.; Ma, J. G.; Jia, S. L.; Jentzen, W.; Medforth, C. J. *Chem. Soc. Rev.* **1998**, *27*, 31–41.
- (73) Choi, J. K.; D'Urso, A.; Balaz, M. J. *Inorg. Biochem.* **2013**, *127*, 1–6.
- (74) Naik, N.; Rubbiani, R.; Gasser, G.; Spingler, B. *Angew. Chem., Int. Ed.* **2014**, *53*, 6938–6941.
- (75) Friedman, A. E.; Chambron, J. C.; Sauvage, J. P.; Turro, N. J.; Barton, J. K. *J. Am. Chem. Soc.* **1990**, *112*, 4960–4962.
- (76) Zeglis, B. M.; Pierre, V. C.; Barton, J. K. *Chem. Commun. (Cambridge, U.K.)* **2007**, 4565–4579.
- (77) Howerton, B. S.; Heidary, D. K.; Glazer, E. C. *J. Am. Chem. Soc.* **2012**, *134*, 8324–8327.
- (78) Angeles-Boza, A. M.; Bradley, P. M.; Fu, P. K. L.; Shatruk, M.; Hilfiger, M. G.; Dunbar, K. R.; Turro, C. *Inorg. Chem.* **2005**, *44*, 7262–7264.
- (79) Aguirre, J. D.; Angeles-Boza, A. M.; Chouai, A.; Pellois, J. P.; Turro, C.; Dunbar, K. R. *J. Am. Chem. Soc.* **2009**, *131*, 11353–11360.